Published in final edited form as:
J Am Chem Soc. 2010 June 23; 132(24): 8385–8397. doi:10.1021/ja101097p.

Site-specific incorporation of 3-nitrotyrosine as a probe of pK_a perturbation of redox-active tyrosines in ribonucleotide reductase

Kenichi Yokoyama[†], **Ulla Uhlin**[§], and **JoAnne Stubbe**[†,‡,*]
Departments of Chemistry and Biology, Massachusetts Institute of Technology, 77 Massachusetts Avenue, Cambridge, MA 02139–4307 and Department of Molecular Biology, Swedish University of Agricultural Science, Uppsala Biomedical Center, Box 590, SE-75124 Uppsala, Sweden

[†]Department of Chemistry, Massachusetts Institute of Technology

[‡]Department of Biology, Massachusetts Institute of Technology

[§]Department of Molecular Biology, Swedish University of Agricultural Science

Abstract

E. coli ribonucleotide reductase catalyzes the reduction of nucleoside 5′-diphosphates into 2′-deoxynucleotides and is composed of two subunits: α2 and β2. During turnover, a stable tyrosyl radical (Y·) at Y_{122}-β2 reversibly oxidizes C_{439} in the active site of α2. This radical propagation step is proposed to occur over 35 Å, to use specific redox-active tyrosines (Y_{122} and Y_{356} in β2, Y_{731} and Y_{730} in α2), and to involve proton-coupled electron transfer (PCET). 3-Nitrotyrosine (NO_2Y, pK_a 7.1) has been incorporated in place of Y_{122}, Y_{731} and Y_{730} to probe how the protein environment perturbs each pK_a in the presence of the second subunit, substrate (*S*), and allosteric effector (*E*). The activity of each mutant is $< 4 \times 10^{-3}$ that of the wt subunit. The [NO_2Y_{730}]-α2 and [NO_2Y_{731}]-α2 each exhibits a pK_a of 7.8 – 8.0 with *E* and *E*/β2. The pK_a of [NO_2Y_{730}]-α2 is elevated to 8.2 - 8.3 in the *S/E*/β2 complex, while no further perturbation is observed for [NO_2Y_{731}]-α2. Mutations in pathway residues adjacent to the NO_2Y that disrut H bonding minimally perturb its *K*a. The pK_a of NO_2Y_{122}-β2 alone or with α2/*S/E* is > 9.6. X-ray crystal structures have been obtained for all NO_2Y-α2 mutants (2.1 – 3.1 Å resolution), which show minimal structural perturbation compared to wt-α2. Together with the pK_a of the previously reported NO_2Y_{356}-β2 (7.5 in the α2/*S/E* complex, Yee, C. et al, *Biochemistry* **2003**, *42*, 14541-14552.), these studies provide a picture of the protein environment of the ground state at each Y in the PCET pathway and are the starting point for understanding differences in PCET mechanisms at each residue in the pathway.

[*]To whom correspondence should be addressed. Tel: (617) 253-1814. Fax: (617) 324-0505. stubbe@mit.edu .
AUTHOR EMAIL ADDRESS: stubbe@mit.edu

SUPPORTING INFORMATION PARAGRAPH (Word Style “TE_Supporting_Information”). SDS-PAGE of purified [NO_2Y]-αs; absorption spectra of [NO_2Y]-α2s in their denatured state; absorption spectra of *N*-acetyl-3-nitrotyrosine amide (0.2 mM) in organic solvent; SDS-PAGE and ESI-QTOF-MS of β expressed in *E. coli* TOP10/pBAD-NrdB-CS(Y356Z)/pEVOL-NO_2Y; UV-vis absorption spectra of [NO_2Y_{122}]-β2 with α2/ATP/CDP; pH titration curves of [NO_2Y]-α2s; the environment of Y_{122} in the crystal structure of wt-β2; pK_as of *o*-, *m*- and *p*-nitrohenol in solution; primers used for cloning and site-directed mutagenesis; crystallographic data collection and refinement statistics; the purity of [NO_2Y]-α2s and β2; λ_{max} of *N*-acetyl-3-nitrotyrosine in organic solvent with 1% triethylamine; Stability of diferric cluster of met-[NO_2Y_{122}]-β2 in basic conditions. This material is available free of charge via the Internet at http://ubs.acs.org.

Introduction

Class Ia ribonucleotide reductases (RNRs) play a crucial role in DNA replication and repair catalyzing the reduction of nucleoside 5′-diphosphates (NDPs) to 2′-deoxynucleoside 5′-diphosphates (dNDPs).[1-3] *E. coli* RNR consists of two homodimeric subunits: α2 and β2. α2 houses the binding sites for substrates (*S*) and effectors (*E*), where *S* is UDP, CDP, ADP or GDP and *E* is ATP, dATP, TTP or dGTP that control the specificity and rate of nucleotide reduction. β2 harbors the radical initiator, a diferric tyrosyl radical (Y_{122}·) cofactor, which reversibly and transiently oxidizes C_{439} in the active site of α2. This thiyl radical initiates nucleotide reduction. The crystal structure of *E. coli* α2[4,5] and of β2[6,7] have been independently solved. A crystal structure of the class Ib RNR from *Salmonella typhimurium* containing both subunits has also been reported at 4.5 Å resolution and may be indicative of an intermediate in the formation of the active RNR complex that has remained elusive.[8] A docking model by Uhlin and Eklund using the structures of α2 and β2 has been generated based on shape complementarity, in which the stable Y_{122}· in β2 is > 35 Å from the C_{439} in α2.[4] This distance is too large for electron tunneling, given the enzyme's turnover number of 1-10 s^{-1}.[9-11] These observations led to the proposal that the radical propagation proceeds by a hopping mechanism through conserved aromatic amino acid residues located in α2 and β2 (Fig. 1).[4,12-15] The present paper reports the site-specific incorporation of the unnatural amino acid 3-nitrotyrosine (NO_2Y) in place of Y_{122} in β2 and Y_{731} and Y_{730} in α2. The studies with these constructs reveal that NO_2Y is an excellent probe of how the protein environment modulates the pK_a of the henol, which is imortant for thinking about the different mechanisms of proton-coupled electron transfer (PCET) between Y_{122} and C_{439}.

Evidence for the radical propagation pathway shown in Fig. 1 has come from a number of different exeriments. Initially, site-directed mutagenesis of each of the conserved aromatic residues on the proposed pathway demonstrated that each is necessary for RNR activity.[13,16,17] However, the inactivity of these mutants recluded further mechanistic investigation. Strong support for the redox role of Y_{356} in β2 was obtained by site-specific incorporation of a variety of tyrosine analogs in place of this residue by the use of exressed protein ligation (EL) methodology. β2 with 3,4-dihydroxyphenylalanine (DOPA) at 356 generated DOPA radical (DOPA·) in a kinetically-competent fashion when incubated with α2/*S* or α2/*S*/*E*.[18] A series of fluorotyrosine analogs (F_nY, n = 2, 3, 4) incorporated into this position allowed modulation of the residue's reduction potential and pK_a,[19,20] both of which lay an important role in PCET.[14,15] Comparison of the activities of $Y_{356}F_nY$-β2s relative to wt-β2 as a function of pH showed that nucleotide reduction could be modulated by reduction potential.[19] In addition, studies with 3,5-F_2Y-β2 showed no obligate coupling between the electron and proton transfer at this residue during radical transport.[21] These results suggest that PCET through Y_{356} involves orthogonal (bidirectional) PCET in which electron and proton are transferred to different acceptors (Fig. 1).[14,15]

Crystallographic data of *E. coli* α2 suggests that PCET within this subunit may occur by a mechanism distinct from that proposed for 356 in β. Y_{731}-, Y_{730}- and C_{439}-α2 are within H bonding distance of one another and the unusual orientation of Y_{731} and Y_{730} relative to one another (Fig. 1) suggests that π–π stacking may occur. This structural insight, in conjunction with theory, has resulted in the proposal of co-linear PCET within α2 in which an electron and a proton are transferred between the same donor/acceptor pair (Fig. 1).[4,12,14,15,22] Radical propagation in α2 has also been investigated by site-specific incorporation of 3-aminotyrosine (NH_2Y) in place of Y_{731}- and Y_{730}- in α by the orthogonal aminoacyl tRNA synthetase (RS)/tRNA method.[23] The NH_2Y residues of [NH_2Y_{731}]-α2 and [NH_2Y_{730}]-α2 in the presence of β2/*S* and β2/*S*/*E* are oxidized to an aminotyrosyl radical (NH_2Y·) in a kinetically competent fashion suggesting that these Y residues are redox active. Recent

studies, in which NH_2Y was incorporated "off-pathway",24 in conjunction with the $Y_{731}NH_2Y$-α2 and $Y_{730}NH_2Y$-α2 studies suggest that radical propagation occurs by a specific pathway.

Several additional results support the proposal of a co-linear PCET (also called hydrogen atom transfer, HAT) mechanism within α. The first is our studies with a photoreactive-Y_{356}R2C19mer peptide complexed to α. This 20mer-peptide, identical to the 20 C-terminal amino acid residues of β including Y_{356}, contains an appended photo-oxidant at its N-terminus. It forms a complex with α2 and makes deoxynucleotides subsequent to light-mediated oxidation of Y_{356}, thus acting as a competent surrogate for the entire β2.25,26 The results with the α mutant Y_{730}F and different photooxidants supports the proton-dependent hopping mechanism.26,27 The second is the observation that [NH_2Y_{731}]- and [NH_2Y_{730}]-α2 and, more recently, [NH_2Y_{356}]-β2 (E. C. Minnihan, and J. Stubbe, unublished results) are active in nucleotide reduction. An energetic analysis of the possible mechanisms of oxidation of C_{439}-α2 by NH_2Y_{730}-α2 supports a hydrogen atom transfer mechanism.23

The experimental data obtained thus far suggest different mechanisms of PCET occur at different residues within the pathway, which in part is a reflection of differences in the protein environment at each site.4,6,14 In order to think about the mechanism of PCET at each site (Fig. 1), a knowledge of the H bonding interactions and pK_a perturbations of each Y within the pathway is necessary.14,15 Given the number of enzymes that utilize a transient Y· in conversion of their substrate to product,1,28 develoment of a method to study the pK_a of a single Y in a protein with many Ys is of general interest.

As a demonstation of its utility, we previously introduced NO_2Y in place of Y_{356} in β2 and showed that its pK_a was perturbed 0.2 pH units in the presence of α2/ADP/dGTP, relative to the pK_a of *N*-acetyl-3-nitrotyrosine amide in aqueous solution.29 We proposed that NO_2Y would be an excellent probe for a several reasons, albeit with some caveats. First, its pK_a of 7.1 is in the middle of the pH range where most proteins, including RNR, are stable. Second, the absorption maximum for its phenol and phenolate at 360 nm and 424 nm, respectively, possess moderately large extinction coefficients and absorption features removed from the protein envelope, facilitating titrations as a function of pH. Finally, in the case of probing redox active Ys, NO_2Y is harder to oxidize than Y by 210 mV at pH 7. Thus in the case of RNR, its incorporation would result in protein incapable of nucleotide reduction due to a block in the pathway, while retaining sensitivity to environmental changes associated with *S* and *E* binding. A drawback associated with the NO_2Y probe is that it can form an intramolecular H bond with the OH of the phenol. Its strength will depend on the orientation of the NO_2 group relative to the plane of the phenyl ring and the hydrophobicity of its environment. Studies of *o*- and *p*-substituted nitrophenols (Table S1) reveal that the *o*-substituted phenols have elevated pK_as relative to the *p*-substituted phenols with the extent of pK_a elevation being dependent on solvent.30-34 The ability to form intramolecular H bonds will undoubtedly perturb reporting on intermolecular H bonding within the protein. However, if the orientation of the NO_2 group remains similar with different mutants, relative pK_as will be informative.

In this work, we have used the NO_2Y-RS/tRNA pair, recently evolved by the Chin and Mehl grous,35 to successfully incorporate NO_2Y in place of Y_{731} and Y_{730} of α2 and Y_{122} of β2. The EPL method, used to incorporate NO_2Y in place of Y_{356}, is not applicable for Y_{731} and Y_{730}, due to the large size of the protein and the buried nature of the backbone of these residues. The pK_a of each of these NO_2Ys (Fig. 1) has been determined in the presence of a single protein subunit and in the α2β2/*E* and α2β2/*E*/*S* complexes. Together with the previously determined pK_a of NO_2Y at 356-β2,29 the data suggest distinct, position-dependent pK_as with minimal perturbations for the three Ys (730, and 731-α2 and 356-β2)

that form transient radicals, compared to the large perturbation at the stable Y· site, Y_{122}. In addition, substrate binding perturbs the pK_a of NO_2Y only at 730. Additional mutations adjacent to the NO_2Y substitution were introduced at positions 731, 730, and 439 in α2, to investigate the effect of the H bonding interactions (Fig. 1) on the pK_a. Minimal effects were observed. Finally, the crystal structures for all the NO_2Y-α2s have been obtained to 2.1 – 3.1 Å resolution and show minimal structural perturbations relative to the wt-α2 crystallized under identical conditions. The NO_2 group is planar with the phenol ring of residue 730 and shows two orientations (planar and perpendicular to the phenol ring) in residue 731. The results of NO_2Y incorporation in these three positions provide the foundation for thinking about differences in mechanism of PCET at different residues in the pathway. The results further demonstrate that NO_2Y is a sensitive reporter on protein environment.

Materials and methods

Luria Bertani (LB) medium, BactoAgar, 100 mm Petri dish plates were obtained from Becton-Dickinson. NO_2Y, M9 salts, ampicillin (Amp), L-arabinose (L-Ara), chloramphenicol (Cm), all amino acids, ATP, 2′-deoxyguanine 5′-trihosphate (dGTP), cytidine 5′-dihosphate (CDP), adenine 5′-diphoshate (ADP), NADPH, ethylenediamine tetraacetic acid (EDTA), Bradford Reagent, Sehadex G-25, phenylmethanesulfonyl fluoride (PMSF) and stretomycin sulfate were purchased from Sigma-Aldrich. Isoproyl-β-D-thiogalactopyranoside (IPTG), dithiothreitol (DTT), *Dpn*I and T4 DNA ligase were from Promega. pBAD/*Myc*-His A, *E. coli* DH5α and TOP10 competent cells, pCR2.1-TOPO, bacterial alkaline phosphatase and oligonucleotides were from Invitrogen. Calf-intestine alkaline phosphatase (CIAP, 20 U/μL) was from Roche. *Nco*I, *Xho*I, *Sal*I, *Bgl*II, *Nde*I and *Pst*I were from New England Biolabs. The purification of *E. coli* thioredoxin36 (TR, 40 units/mg), *E. coli* thioredoxin reductase37 (TRR, 1400 units/mg), and wild-tye (wt) β238 (6200-7200 nmol/min/mg, 1-1.2 radicals per β2) and wt α239 (2300-2600 nmol/min/mg) have previously been described. The concentrations of α2 and [NO_2Y]-α2s were determined using ε_{280nm} = 189 mM^{-1} cm^{-1}.40 The concentrations of β2 and [NO_2Y_{122}]-β2 were determined using ε_{280nm} = 131 mM^{-1} cm^{-1}.40 The concentrations of apo-[NO_2Y_{122}]-β2 were determined using ε_{280nm} = 120 mM^{-1} cm^{-1}.41 Glycerol minimal media leucine (GMML)42 contains final concentrations of 1% (v/v) glycerol, 1×M9 salts, 0.05% (w/v) NaCl, 1 mM $MgSO_4$, 0.1 mM $CaCl_2$, and 0.3 mM L-leucine. RNR assay buffer consists of 50 mM HEPES, 15 mM $MgSO_4$, 1 mM EDTA, pH 7.6. UV-vis absorption spectra and the spectrophotometric assays were carried out using the Cary 3 UV-vis Spectrophotometer (Varian, Walnut Creek, CA). The Ultramark EX Microlate Imaging System (BioRad) was used to determine A_{280nm} for protein, A_{340nm} for diferric cluster and NO_2Y phenol, A_{490nm} for NO_2Y phenolate of fractions after column chromatograhy. All DNA sequences were confirmed by the MIT Biopolymers Laboratory. PCR was carried out using PfuUltraII polymerase (Stratagene) according to the manufacturer's protocol. The annealing temperature and number of cycles varied are described individually. For site-directed mutagenesis, PCR was performed for 18 cycles with annealing temperature of 55°C, followed by *Dpn*I digestion of methylated template plasmid. The primers used for PCR are summarized in Table S2. pSUP-3NT/835 was kindly supplied by Dr. J. W. Chin (Medical Research Council Laboratory of Molecular Biology, Cambridge, U.K.) and Dr. R. A. Mehl's lab (Franklin & Marshall College, Lancaster) and pEVOL43 was a kind gift of Dr. P. G. Schultz (The Scripps Research Institute, San Diego).

Construction of pBAD-*nrdA*-$Y_{730}Z$ and BAD-*nrdA*-$Y_{731}Z$

nrdA was amplified by PCR using pMJ1-*nrdA*44 as a template with primers, nrdA-f and nrdA-r (Table S2) that harbor *Nco*I and *Xho*I restriction sites, respectively. Intproduction of the *Nco*I site changed the first base of the second codon, A to G, which mutated the second

amino acid, Asn to Asp. PCR was carried out as described above for 40 cycles with an annealing temperature of 58°C. The product was digested with *Nco*I and *Xho*I and sub-cloned into pBAD/*Myc*His-A to give pBAD-*nrdA*. The TAG codon (Z) was inserted at 730 or 731 using primers Y730Z-f and Y730Z-r for 730, and Y731Z-f and Y731Z-r for 731 (Table S2). The mutation accompanied by *Nco*I site intproduction in the first PCR was repaired using primers nrdA-repair-f and nrdA-repair-r (Table S2) to give pBAD-*nrdA*-$Y_{730}Z$ and pBAD-*nrdA*-$Y_{731}Z$.

Construction of EVOL-NO_2Y

pEVOL43 carries two copies of an RS gene, one with *Sal*I and *Bgl*II sites and the other with *Nde*I and *st*I sites in the upstream and downstream regions of the gene, respectively. *Sal*I and *Bgl*II sites were introduced into the 3-nitrotyrosine RS (NO_2Y-RS) gene by PCR using pSUP-3NT/835 as a template and primers RS-f and RS-r (Table S2). PCR was carried out for 30 cycles with an annealing temperature of 55°C. Adenine was then added to the 3′-terminus of the PCR product for TA ligation by incubation with GO-Taq Hot start polymerase (Promega) in the presence of 0.2 mM dATP at 72°C for 30 min. The product was ligated with PCR2.1-TOPO (Invitrogen) following the manufacturer's protocol. The resulting plasmid was first digested with *Bgl*II and a 3.9 kb DNA fragment containing NO_2Y-RS gene was isolated and further digested with *Sal*I. The second NO_2Y-RS gene with *Nde*I and *Pst*I sites was prepared by digesting pSUP-3NT/8 with *Nde*I and *Pst*I. The two NO_2Y-RS gene fragments were sequentially introduced into pEVOL. Initially, the NO_2Y-RS gene flanked by *Nde*I/*Pst*I was ligated into pEVOL. The NO_2Y-RS gene flanked with *Bgl*II/*Sal*I was then ligated into the new construct to give pEVOL-NO_2Y.

Expression of [NO_2Y_{730}]-α2 and [NO_2Y_{731}]-α2

E. coli TOP10 was transformed with pSUP-3NT/835 (Cm^R) and pBAD-*nrdA*-$Y_{730}Z$ and grown overnight on LB agar plates. All growths were carried out in the presence of Cm (25 mg/L) and Amp (100 mg/L). A single colony was picked and grown in LB to saturation (~16 h). Two mL of this solution was diluted into 200 mL LB in a 500 mL baffled flask and grown at 37°C until saturation. A portion of this culture (100 mL) was then inoculated into a fermenter containing 10 L of GMML medium (pH 6.8) supplemented with Cm (25 mg/L), Amp (100 mg/L), 17 amino acids (Glu, Gln, Asp, Asn, Lys, Val, Arg, Leu, His, Ile, Ala, Pro, Trp, Gly, Met, Thr, Ser, 0.2 g/L each), D-glucose 0.05% (w/v), Asp 0.25% (w/v), L-ara 0.1% (w/v) and 1X heavy metal solution. The heavy metal stock solution (1000X) contained the following per L:45 500 mg of $Na_2MoO_4{\cdot}2H_2O$, 250 mg of $CoCl_2$, 175 mg of $CuSO_4{\cdot}5H_2O$, 1 g of $MnSO_4{\cdot}H_2O$, 8.75 g of $MgSO_4{\cdot}7H_2O$, 1.25 g of $ZnSO_4{\cdot}7H_2O$, 1.25 g of $FeCl_2{\cdot}4H_2O$, 2.5 g of $CaCl_2{\cdot}2H_2O$ and 1 g of H_3BO_3, dissolved in 1 M HCl. NO_2Y (2 mM) was added at the beginning of the culture and growth was continued for 30 h (OD_{600} = 2.6 – 2.8) at which time the cells were harvested by centrifugation, frozen in liquid N_2 and stored at −80°C. Typically, 5-6 g of wet cell paste/L were obtained. Expression of [NO_2Y_{731}]-α2 and all double mutants were carried out in an identical fashion using the appropriate pBAD constructs.

Purification of [NO_2Y_{730}]-α2 and [NO_2Y_{731}]-α2

[NO_2Y]-α2s were typically purified from 60-80 g of cell paste. All purification steps were carried out at 4°C. The cell paste was re-suspended in 5 volumes of buffer A (50 mM Tris pH 7.6, 1 mM EDTA, 1 mM PMSF and 5 mM DTT). The cells were lysed by a single passage through a French pressure cell operating at 14 000 psi. After removal of cell debris by centrifugation (20000*g*, 20 min, 4°C), DNA was precipitated by dropwise addition of 0.2 volumes of buffer A containing 8% (w/v) streptomycin sulfate. The mixture was stirred for an additional 15 min, and the precipitated DNA was removed by centrifugation (20000*g*, 20

min, 4°C). Solid $(NH_4)_2SO_4$ (3.9 g per 10 mL of supernatant) was then added over 15 min (66% saturation). The solution was stirred for an additional 20 min and the precipitated protein was isolated by centrifugation (20000*g*, 20 min, 4°C). The pellet was dissolved in a minimal volume of buffer A and desalted using a Sephadex G-25 column (5 cm × 50 cm, 1 L). The desalted protein was loaded onto DEAE Fast Flow column (7 cm × 14 cm, 500 mL), which had been equilibrated in buffer A. The column was washed with 2 L of buffer A containing 50 mM NaCl followed by a gradient (1 L × 1 L) of 50-500 mM NaCl in buffer A. Fractions (10 mL each) containing [NO_2Y]-α2 were judged by SDS-PAGE and differences of phenolate absorption (A_{490nm}) at pH 7.6 and 9.0. [NO_2Y]-α2 was typically eluted at 210-250 mM NaCl. Pooled fractions were then directly loaded onto a dATP affinity column46 (1.5 cm × 4 cm, 100 mL), which had been equilibrated in buffer A. The column was washed with 10 column volumes of buffer A. [NO_2Y]-α2 was then eluted with buffer B (50 mM Tris pH 7.6, 5% glycerol, 1 mM EDTA, 15 mM $MgSO_4$, and 5 mM DTT) supplemented with 5 mM ATP and 5 mM DTT. Fractions containing NO_2Y-α2, judged by SDS-PAGE, were pooled and concentrated by ultrafiltration (Amicon YM-30, Millipore) and loaded onto Q-sepharose HP (Sigma-Aldrich, 3 × 5 cm, 35 mL), which had been equilibrated in buffer C (50 mM Tris pH 8.0, 5% glycerol, 1 mM EDTA, 15 mM $MgSO_4$, and 5 mM DTT). The column was washed with buffer C containing 50 mM NaCl and 1 mM ATP. ATP was added to revent equilibration between the monomer and dimer of α, which results in the protein eluting over a larger volume. The protein was eluted using a gradient (300 mL × 300 mL) of 50-500 mM NaCl in the same buffer. Fractions containing [NO_2Y]-α2 (typically, 160 - 210 mM NaCl), judged by SDS-PAGE, were then concentrated by ultrafiltration as above and desalted using a Sephadex G-25 column (1.1 × 100 cm, 100 mL) equilibrated with buffer B. The resultant protein solution was concentrated to ~90 μM, frozen in liquid N_2, and stored at −80°C. Typically, 1-3 mg of [NO_2Y]-α2s were obtained per g of wet cell paste.

Generation and exression of [NO_2Y_{122}]-β2

A TAG codon was introduced by PCR using pBAD-*nrdB*-NS547 as a template and primers, Y122Z-f and Y122Z-r (Table S2). NrdB encoded in pBAD-*nrdB*-NS5 has a StrepII tag (WSHPQFEK) at its N-terminus followed by a 5 amino acid linker (SLGGH). The resulting plasmid, pBAD-*nrdB*-NS5-Y_{122}Z (Amp^R), was introduced into *E. coli* TOP10 together with pEVOL-NO_2Y (Cm^R) and grown overnight on LB agarose plates. All growths were carried out in the presence of Cm (25 mg/L) and Amp (100 mg/L). A single colony was picked and grown in 5 mL LB to saturation (~16 h). Two mL of this solution was diluted into 200 mL LB in a 500 mL baffled flask and grown at 37°C until saturation (~10 h). A portion of this culture (100 mL) was then inoculated into a fermenter containing 10 L of the 17 amino acids supplemented GMML medium described above. NO_2Y (2 mM) was added at the beginning of the culture and growth was continued for 15 h (OD_{600} = 1.5-1.8) at which point the cells were harvested by centrifugation, frozen in liquid N_2 and stored at −80°C. Typically, 2-3 g of wet cell paste/L were obtained.

Purification of [NO_2Y_{122}]-β2

[NO_2Y_{122}]-β2 was purified from 30-40 g wet cell paste. Although the [NO_2Y_{122}]-β2 is strep-tagged, the standard protocol38 for β2 purification was used for large scale preparations due to the poor binding of tagged [NO_2Y_{122}]-β2 to *Stre*-Tactin sepharose (IBA, St. Louis, MO). All steps were carried out at 4°C. The cell paste was re-suspended in 5 volumes of buffer D (50 mM Tris pH 7.6, 5% glycerol and 0.5 mM PMSF). The cells were lysed by a single passage through a French pressure cell operating at 14,000 psi. $Fe^{II}(NH_4)_2(SO_4)_2$ and sodium ascorbate (5 mg each per g cell paste) were added to the lysate and stirred for 10 min. After removal of cell debris by centrifugation (20000*g*, 20 min,

4 °C), DNA was precipitated by drowise addition of 0.2 volumes of buffer D containing 6% (w/v) streptomycin sulfate. The mixture was stirred for an additional 15 min, and the precipitated DNA was removed by centrifugation (20000*g*, 20 min, 4°C). Solid $(NH_4)_2SO_4$ (3.9 g er 10 mL of supernatant) was then added over 15 min (66% saturation). The solution was stirred for an additional 20 min and the precipitated protein was isolated by centrifugation (20000*g*, 20 min, 4°C). The pellet was dissolved in a minimal volume of buffer D and desalted using a Sehadex G-25 column (5 cm × 50 cm, 1 L). The desalted protein was loaded onto DEAE Fast Flow column (5 cm × 13 cm, 250 mL), which had been equilibrated in buffer D. The column was washed with 1.5 L of buffer D containing 100 mM NaCl followed by a gradient (1 L × 1 L) of 100-500 mM NaCl in buffer D. Fractions containing $[NO_2Y_{122}]$-β2 were judged by SDS-PAGE and A_{340nm}, the absorption feature of diferric cluster and 3-nitrophenol. $[NO_2Y_{122}]$-β2 typically eluted at 190 – 220 mM NaCl. The resulting fractions were then diluted two-fold using buffer D and were loaded onto a Q-sepharose fast flow column (4.5 cm × 10 cm, 150 mL), which had been equilibrated in buffer D. The column was washed with 1.5 L of buffer D containing 150 mM NaCl followed by a gradient (1 L × 1 L) of 150-500 mM NaCl in buffer D. Fractions containing $[NO_2Y_{122}]$-β2 (220-250 mM NaCl), judged by SDS-PAGE, were pooled and concentrated by ultrafiltration (Amicon YM-30, Millipore) to ~500 μM, frozen in liquid N_2, and stored at −80°C. Typically, 7 mg of $[NO_2Y_{122}]$-β2 were obtained per g of wet cell paste. The iron content was determined by the ferrozine assay.48

For activity assays, *Strep*-Tactin sepharose (IBA, St. Louis, MO) was used to remove contaminating wt-β2 from $[NO_2Y_{122}]$-β2. Typically 4-5 g of cell paste was used. Cell lysis, stretomycin sulfate precipitation and ammonium sulfate precipitation were carried out as described above. After removal of ammonium sulfate using Sephadex G-25, the desalted protein was loaded onto *Strep*-tactin sepharose column (1 cm × 5 cm, 4 mL), which had been equilibrated in buffer D. The column was washed with buffer D and $[NO_2Y_{122}]$-β2 was eluted with 2.5 mM desthiobiotin in buffer D. Typically, 0.4 mg of $[NO_2Y_{122}]$-β2 was obtained per g of wet cell paste. The decreased yield is due to a low affinity of $[NO_2Y_{122}]$-β2 for the resin. protein concentration and iron content were determined as described above.

Generation and expression of double mutants: $[NO_2Y_{730}]$-α2(Y_{731}F), $[NO_2Y_{730}]$-α2(Y_{731}A), $[NO_2Y_{730}]$-α2(C_{439}S), $[NO_2Y_{730}]$-α2(C_{439}A), and $[NO_2Y_{731}]$-α2(Y_{730}F)

Mutations were introduced by PCR as described above with primers in Table S2. pBAD-*nrdA*-Y_{730}Z was used as a template for $[NO_2Y_{730}]$-α2(Y_{731}F), $[NO_2Y_{730}]$-α2(Y_{731}A), $[NO_2Y_{730}]$-α2(C_{439}S) and $[NO_2Y_{730}]$-α2(C_{439}A), and pBAD-*nrdA*-Y_{731}Z was used as a template for $[NO_2Y_{731}]$-α2(Y_{730}F). PCR products were amplified in *E. coli* DH5α and their DNA sequences were confirmed. Expression and purification of these proteins were carried out as described above for NO_2Y-α2 single mutants.

Determination of protein purity and NO_2Y incorporation

The purity of each $[NO_2Y]$-α2 and $[NO_2Y]$-β2 was determined from SDS-PAGE and Coomassie staining using Quantity One software (BioRad). The amount of NO_2Y incorporated into α2 or β2 was determined by its phenolate absorption subsequent to its incubation in 6 M guanidine in 50 mM TAS pH 9.0 at room temperature for 1 h. The measurement was repeated in trilicate. *N*-acetyl-3-nitrotyrosine amide, prepared as previously described29 and recrystallized from methanol, was used as a standard. The solvent was removed in vacuo over P_2O_5 for 18 h, until no further changes in weight were

observed. The extinction coefficient of *N*-acetyl-3-nitrotyrosine amide was determined by weight and UV-vis spectrum.

K_D for the interaction of β2 and [NO_2Y]–α2s in the presence of CDP/ATP by the cometitive inhibition assay.49

The assay mixture in a final volume 300 μL consisted of 0.15 μM β2, 1 mM CDP, 1.6 mM ATP, 50 μM TR, 1 μM TRR, 0.2 mM NADH in RNR assay buffer. The reaction was initiated by adding a mixture of 0.3 μM wt α2 and variable amounts of [NO_2Y]-α2s (0, 0.1, 0.2, 0.5, 1.0, 2.0, 4.0 μM) and the A_{340nm} (ε = 6.22 $mM^{-1}cm^{-1}$), corresonding to NADPH consumtion, was monitored at 25°C. The data were fit to eq. 1.

$$[NO_2Y-\alpha 2]_{bound}=[\alpha 2\beta 2]_{max}\times[NO_2Y-\alpha 2]_{free}/(K_d+[NO_2Y-\alpha 2]_{free}) \quad \text{eq.1}$$

where $[NO_2Y\text{-}\alpha2]_{bound}$ is the concentration of the NO_2Y-α2β2 complex, $[\alpha2\beta2]_{max}$ is the concentration of the wt-α2β2 complex in the absence of [NO_2Y-α2], and K_d is the dissociation constant of [NO_2Y]-α2 from β2. $[\alpha2\beta2]_{max}$ was 0.09 μM under these assay conditions. Each data point represents an average of three independent measurements. The K_d for the subunit interaction between α2 and [NO_2Y_{122}]-β2 was measured in the identical manner using 0.15 μM wt α2 and 0.3 μM wt β2.

Spectrophotometric and Radioactive Activity Assays

The spectrophotometric and radioactive RNR assays were performed as described.29 Typically, [NO_2Y]-α2s (1 or 2 μM), wt β2 (2, 5 or 10 μM) was incubated with CD (1 mM), ATP (3 mM) in the presence of TR, TRR and NADH in RNR assay buffer. [5-^{3}H]-CDP (5150 - 5230 cpm/nmol, ViTrax, Placentia, CA) was used in the radioactive assay.

Determination of the pK_a of NO_2Y in [NO_2Y]-α2s and [NO_2Y_{356}]-β2 in the presence of *E, E*/β2 (or α2) and *E*/β2(or α2)/*S*

To determine the pK_a of NO_2Y in the α2 mutants, the absorption spectra from 250 to 700 nm were determined at 25 °C at each pH. Each step in the titration was carried out in a separate cuvette. Good's buffers (50 mM, MES (pH 6.0 – 6.8), HEPES (pH 7.0 – 8.0), and TAPS (pH 8.2 – 9.2) contained 1 mM EDTA and 15 mM $MgSO_4$. Each buffered solution contained: [NO_2Y]-α2 (7.5 μM) and *E* (ATP or dGTP at 1 mM and 0,1 mM, respectively), *E*/β2 (7.5 μM), or *E*/β2/*S* (CDP or ADP at 1 mM). The pH was redetermined after mixing all components. To compensate for differences in baseline absorption, all spectra were zeroed at 700 nm. All titrations were conducted in triplicate. Analysis of the titration data was carried out using eq.2,

$$A=(\varepsilon_H K_a[H^+]+\varepsilon^-)[NO_2Y-\alpha]/(K_a[H^+]+1) \quad \text{eq.2}$$

where *A* is the absorbance of the phenolate, ε^- is the extinction coefficient of phenolate at its λ_{max}, and ε_H is the extinction coefficient of the phenol at the same wavelength as the phenolate λ_{max}. The data from the lot of *A* vs pH was fit to eq.2 using Kaleidagraph and non-linear least squares curve fitting to determine ε_H, ε^- and pK_a.

[NO_2Y_{356}]-β2, previously prepared by EPL29 was used to determine the pK_a in the complex with α2/ATP/CDP. The titration was carried out as described above, in the presence of *E*/α2 (1 mM ATP, 7.5 μM α2), or *E*/α2/*S* (1 mM CDP). The data were fit to eq.2 to determine the pK_a.

pH titration of NO_2Y in [NO_2Y_{122}]-β2

The absorption spectrum of [NO_2Y_{122}]-β2 was determined between pH 7.0 and 10.6 at 25 °C as above. For a pH higher than 9.0, CHES (pH 9.0 – 10.0) and CAPS (pH 10.3 – 10.6) were used. Titrations were carried out with [NO_2Y_{122}]-β2 (7.5 μM), with [NO_2Y_{122}]-β2(7.5 μM)/α2(7.5 μM)/ATP(1 mM)/CDP (1 mM), or with apo-[NO_2Y_{122}]-β2 (7.5 μM). The pH was measured after mixing all components. To compensate for differences in baseline absorption, all spectra were zeroed at 700 nm. Ao-[NO_2Y_{122}]-β2 was prepared using hydroxyquinoline as a chelator in the presence of 1 M imidazole.41

Crystallization, data collection and refinement

Wt-α2 and [NO_2Y]-α2s were co-crystallized with a 20mer peptide4 that corresponds to the last 20 amino acids of β2. Crystals were grown for approximately one week at 4 °C using the hanging drop vapor diffusion method in EasyXtal Tool plates (QIAGEN). Each drop consisted of 2 μL α-mutant (8-9 mg/ml) and peptide (30 mg/ml) and 2 μL of a solution containing 1.5 M Li_2SO_4, 2 mM DTT and 25 mM sodium citrate (pH 6). The final pH of each drop was 6.0-6.5. The crystals were quickly washed in a 1.5 M Li_2SO_4 solution containing 20% ethylene glycol, mounted in fiber loops and flash-frozen in liquid N_2.

All sets of data were collected at 100 K at the European Synchrotron Radiation Facility stations (Grenoble, France). The crystals are of the rhombohedral space group R32 with hexagonal axes approximately 225, 225 and 337 Å, containing 3 molecules per asymmetric unit. Due to the freezing of the crystals, the cells are slightly smaller than the previous data of wt-α2 collected at 4 °C.4 $Y_{730}F$-α2 coordinates5 (DPB ID, 1R1R) were used as an initial model in refinement of the wt-α2 data (2.3 Å resolution). This wt-α2 structure was then used as a starting model for all [NO_2Y]-α2s. To verify the positions of modifications/mutations, difference maps between the new wt-α2 structure and each [NO_2Y]-α2 structure were inspected after the first restrained cycle of refinement. Table S3 summarizes the details of data collection and refinement.

Results

Incorporation of NO_2Y into α2

The Chin and Mehl groups35 recently reported the evolution of a suppressor tRNA/RS pair for site-specific incorporation of NO_2Y into superoxide dismutase (SOD) expressed in *E. coli*. Initially their construct pSUP-3NT/8, containing the genes for both the tRNA and the RS was used in combination with pTrc containing *nrdA* (the gene for RNR α) with the TAG codon in place of the tyrosine codon at 730 or 731. pTrc plasmid has recently been successfully used by us to incorporate NH_2Y into the same positions of α2.23 Expression was carried out in GMML medium42 or in the minimal medium used for NO_2Y incorporation into SOD.35 Under these conditions, however, only very weak expression of truncated α2 was observed. In an effort to enhance expression of α, we cloned *nrd*A into pBAD/*Myc*His-A to generate pBAD-*nrdA* and attempted expression in richer medium.50 *E. coli* TOP10 cells were transformed with pSUP-3NT/8 and pBAD-*nrdA*-$Y_{730}Z$ or pBAD-*nrdA*-$Y_{731}Z$ and grown in GMML medium containing NO_2Y, D-glucose, L-ara and 17 proteinogenic amino acids excluding Cys, Tyr and Phe. Under these conditions, protein expression was robust, giving rise to predominantly truncated α and a small amount of full-length protein (Fig. 2a, left gel). Fortunately, most of the truncated protein was insoluble, and thus full-length α was successfully isolated by our standard procedure for α purification which uses a dATP affinity column,46 followed by an additional Q Sepharose column (Fig. S1). Typically 2.8 mg of [NO_2Y_{730}]-α2 and 1.0 mg of [NO_2Y_{731}]-α2 are isolated per g of cell paste. More recently we have used the newly constructed pEVOL-NO_2Y (see below) that results in higher expression levels of full length [$NO_2Y730(731)$]-α2 (Fig. 2a, right gel).

The purity of [NO_2Y_{730}]-α2 and [NO_2Y_{731}]-α2 was determined to be ~95% and ~80%, respectively, based on the intensities of the Coomassie stained protein bands on SDS-PAGE gel (Fig. S1 and Table S4). At pH 9.2, these mutants exhibit a phenolate λ_{max} of 442 nm and 437 nm, respectively, which is red-shifted 18 nm and 13 nm from the phenolate λ_{max} of *N*-acetyl-3-nitrotyrosine amide29 (424 nm) in the same buffer (Fig. 3a). To calculate the extent of NO_2Y incorporation into α, each [NO_2Y]-α2 was denatured in 6 M guanidine HCl in 50 mM TAS pH 9.2. Both denatured mutants exhibited a phenolate λ_{max} of 435 nm, identical to that of the *N*-acetyl-3-nitrotyrosine amide in the same buffer (Fig. S2).51 The extinction coefficient (ε_{435nm}) of *N*-acetyl-3-nitrotyrosine amide in 6 M guanidine (pH 9.2) was determined to be 4890 $M^{-1}cm^{-1}$.51 By measuring A_{435nm} of the denatured [NO_2Y]-α2s, the concentration of NO_2Y in each mutant was determined. These numbers allowed the determination of the purity of [NO_2Y_{730}]-α2 and [NO_2Y_{731}]-α2 to be 93 ± 3% and 79 ± 3%, respectively, which correlate well with the purity of α2 determined from SDS-PAGE analysis (Table S4), suggesting that the impurity is associated with other proteins and that incorporation of NO_2Y into both [NO_2Y]-α2s, is high (98 ± 2%).

Incorporation of NO_2Y into β2

In contrast with the results using pSUP-3NT/8 for the incorporation of NO_2Y into α, efforts to exress full-length β with NO_2Y at 122 were unsuccessful, desite detection of substantial amounts of truncated protein. Recently, the Schultz group has develoed a new plasmid, pEVOL, in which aminoacyl-RS expression is controlled by the strong ara inducible promoter, *ara*BAD.43 pEVOL has been demonstrated to improve suppression relative to other constructs in a number of cases.43 Thus, the NO_2Y-RS was cloned into pEVOL resulting in pEVOL-NO_2Y and used to examine NO_2Y incorporation in place of Y_{122} in β2. Successful expression of full-length β2 was observed when the protein was expressed in the amino acid supplemented minimal medium using pEVOL-NO_2Y and pBAD-*nrdB*-NS5-$Y_{122}Z$ (Fig. 2b). pBAD-*nrdB*-NS5-$Y_{122}Z$ encodes β with *Strep*II tag and a 5 amino acid linker (SLGGH) at the N-terminus and a TAG codon (Z) at position 122. We have previously confirmed that the N-terminal *Strep*-tag does not affect the RNR activity.47 *Strep*-tagged β2 will be referred to as β2. Attempts to purify [NO_2Y_{122}]-β2 with the *Strep*-tactin affinity resin were inefficient due to poor binding, yielding 0.4 mg β2 per g cell-paste. Thus, [NO_2Y_{122}]-β2 was purified by our standard procedure for non-tagged β2 using anion exchange column chromatograhy. Typically 6-7 mg [NO_2Y_{122}]-β2 per g cell paste with 90% purity based on SDS-PAGE gel analysis, was obtained (Fig. 2b, Table S4).

As isolated, the absorption spectrum of the purified [NO_2Y_{122}]-β2 showed broad features between 325 and 400 nm and no sharp feature associated with a Y· at 410 nm (Fig. 3b). The ferrozine assay revealed 2.9 ± 0.2 Fe/β2, suggesting that [NO_2Y_{122}]-β2 has a diferric cluster (met-form). Thus, if $NO_2Y\cdot$ is formed, it is short-lived. Incorporation of NO_2Y was confirmed to be ~98% as described above for α (Table S4). Subtraction of the absorption spectrum of the diferric cofactor cluster (normalized for the iron content) from that of [NO_2Y_{122}]-β2 gave a spectrum with a λ_{max} at 363 nm (ε = 3400 ± 240 $M^{-1}cm^{-1}$, Table 1, Fig. 3b), consistent with a phenol form of NO_2Y.

Finally, incorporation of NO_2Y in place of Y_{356} was also attempted. Since the truncated β was soluble, C-terminal *Strep*-tagged β47 was used to facilitate the searation of full-length β from truncated β. The use of pEVOL-NO_2Y and pBAD-NrdB-$Y_{356}Z$ resulted in expression of full-length β that was not observed when the protein was expressed in the absence of NO_2Y (Fig. S3). However, the purified full-length β did not exhibit the phenolate absorption at pH 9.2 under native or denaturing conditions, suggesting the absence of NO_2Y incorporation. An ESI-MS analysis showed the purified β has a molecular mass 15 Da larger than the wt protein (Fig. S4), which corresponds to an addition of an NH_2 group. No signal corresponding to [NO_2Y_{356}]-β2 was observed. Previous workers have reported that NO_2Y

can be reduced to NH_2Y by heme proteins in the presence of thiols or ascorbic acid.52 Since residue 356 is surface exposed, it is likely to have been reduced in *E. coli* cells.

Determination of the K_d for Subunit interactions

The K_d for subunit interactions in wt-RNR is weak [0.06 -0.2 μM in the presence of CDP and ATP,49 (A. Q. Hassan and J. Stubbe, unpublished results) and 0.4 μM in the absence of nucleotides54]. Perturbation of subunit interactions by NO_2Y incorporation was thus a concern as 731 is thought to reside at the subunit interface. Thus, the K_d was determined by the procedure of Climent et al49, using the [NO_2Y]-α2s and [NO_2Y_{122}]-β2 as a competitive inhibitor of wt-α2 and -β2 interactions. This method gave a K_d of 1.32 ± 0.10 μM, 0.51 ± 0.07 μM and 0.40 ± 0.06 μM for [NO_2Y_{730}]-α2, [NO_2Y_{731}]-α2 and [NO_2Y_{122}]-β2, respectively (Table 2). Since the formation of the phenolate of NO_2Y could perturb subunit interactions, the K_d was also determined at pH 6.8 where the phenol is comletely protonated. The observed K_d for [NO_2Y_{731}]-α2 (0.53 ± 0.07 μM) is essentially the same as that at pH 7.6. In general, the interactions are weaker than those observed in wt RNR. Unexectedly, the K_d of [NO_2Y_{730}]-α2 is higher than that of [NO_2Y_{731}]-α2, even though Y_{731}-α2 is closer to the subunit interface.4 This knowledge facilitated design of studies, pK_a determination and activity assays, where the subunits need to be associated.55

Catalytic activity of NO_2Y-α2s: levels of endogenous wt-α

The genes for RNR are essential and therefore expression of [NO_2Y]-β or [NO_2Y]-α mutants in *E. coli* is accompanied by expression of small amounts of the endogenous wt-subunit. The purification protocol for [NO_2Y_{356}]-β2 made by EPL ensured the removal of wt-β and thus a lower limit of detection of deoxynucleotide formation for this mutant of < $1/10^4$ that of wt-β2 was set.29 The absence of activity was exected based on the experimentally measured differences in peak potentials of the NO_2Y and Y of 210 mV (pH 7.6)29 and our previous studies with F_nY (n = 2-4) at the same position, which suggested that when the F_nY was more difficult to oxidize than Y by 200 mV, RNR was inactive.20

Activity of [NO_2Y_{122}]-β2 with an *N*-terminal *Strep*-tag and without a tag, purified by affinity chromatography and by conventional chromatography methods, respectively, was determined. In the former case, the [NO_2Y_{122}]-β2 had activity 1/250 and in the latter case < $1/10^4$ of the wt-β2 (Table 3). Thus, [NO_2Y_{122}]-β2 is inactive.

The activity assays of [NO_2Y_{730}]- and [NO_2Y_{731}]-α2, Table 3, revealed activity levels of 0.5 – 1.5% for [NO_2Y_{730}]-α2 (1/200 to 1/100) to 0.4 - 2.9% for [NO_2Y_{731}]-α2(1/250 to 1/30) that of wt-α2. Three arguments support our conclusion that the observed activity is predominantly associated with endogenous wt-α. First there is a rough correlation between the levels of expression of the mutants and their activity (Table 3): the higher the yield of the mutant protein, the lower the activity. Expression of [NO_2Y_{731}]-α, for examle, with two different suppression constructs gives rise to activity that varies 5 fold. Second, a number of double mutants, described below, with NO_2Y and a block (he) in the ET pathway, all have activities in the range of 1 to 3% (1/30 to 1/100) of wt. The Phe mutants themselves have been deemed inactive with similar levels of activity.13 Third, the activity measured for [NO_2Y]-α2 assayed at 2 μM is independent of the concentration of β2 (2 μM, 5 μM or 10 μM) used in the assay mixture. Based on the K_d for subunit interactions, the RNR activity would have been exected to increase with the increasing concentrations of β2 due to increased α2β2 complex formation.55

Finally, we have recently developed an affinity chromatography method to remove endogenous levels of wt-α2 from [NH_2Y]-α2s by constructing an N-terminally tagged α, into which the unnatural amino acid is incorporated (E. C. Minnihan, and J. Stubbe,

unublished results). Use of this construct to generate [NO_2Y_{730}]-α2 gave protein of 92% purity and activity 0.5% that of wt-α2 at pH 7.6. The activity is also 0.50 ± 0.02% that of wt-α at pH 6.5 and 8.6. If the mechanism of oxidation of C_{439} involves hydrogen atom transfer, then at pH 8.6 the relative activity should be reduced to <25% of that at pH 6.8, as the NO_2Y is predominantly the phenolate at pH 8.6 (see titration data below and Table 4). From the arguments presented above we have assumed that all the [NO_2Y]-α2s and β2s are inactive and that the detected activity is associated with endogenous wt-α or with the infidelity of the RS associated with mischarging the tRNA with Y.

Determination of the pK_as of [NO_2Y]-α2s

The ability to form [NO_2Y]-α2β2 complexes incapable of turnover has enabled us to determine the pK_a of NO_2Y at positions 730 and 731 in α2 in the presence *S* (ADP or CDP) and *S/E* air (CDP/ATP or ADP/dGTP). As noted above, *S* and *E* are critical as they trigger the active conformation for PCET. The pH measurements of the α2β2 complex were performed between pH 6.0 – 9.2 with [NO_2Y]-α2 and β2 in which 65% of [NO_2Y_{730}]-α2 and 77% of [NO_2Y_{731}]-α2 are in a complex based on the K_d (Table 2). An additional experiment was carried out with 92% complex formation with similar results. The errors in the pK_a values were ± 0.05 pH units. The protein stability was also ascertained at the two pH extremes (6.0 and 9.2) by incubating the wt RNR at these pH for 15 min followed by an activity assay at pH 7.6. In each case 95% of the activity was retained. The results of a tyical pH titration in the presence of *E* are shown in Fig. 4. As the pH increases, the absorption of the phenol decreases concomitant with an increase in the absorption of the phenolate with an isosbestic point at 393 nm. Plots of the intensity of the phenolate absorption vs pH are shown in Fig. 5. The data is best fit to eq.229 for a species undergoing a single deprotonation. The pK_as of NO_2Y in each [NO_2Y]-α2 are summarized in Tables 4A and 4B and can be compared to the pK_a 7.1 for NO_2Y in the C-terminal 20mer peptide of β2.29 The pK_a of [NO_2Y_{730}]-α2 with *E* is 7.9 and 7.8 for ATP and dGTP, respectively. These pK_as remain unchanged uon addition of β2. Addition of *S* to the [NO_2Y_{730}]-α2/*E*/β2 complex, either a purine or a pyrimidne, increased the p$K_a$by 0.4 pH units. The pK_a of NO_2Y at 731 is similar to 730 when titrated with *E* or *E*/β2, however, no further change is observed on *S* addition.

The extinction coefficients for the phenolate of each NO_2Y in α2 were also determined by fits to eq. 2 and are 6400 ± 250 and 5200 ± 300 $M^{-1}cm^{-1}$ for [NO_2Y_{730}]-α2 and [NO_2Y_{731}]-α2, respectively (Table 1). These values are larger than those determined for *N*-acetyl-3-nitrotyrosine amide under the same conditions (λ_{max} 424 nm, ε_{424nm} 4610 $M^{-1}cm^{-1}$). The extinction coefficients of phenols were also calculated from the absorbance at λ_{max} at pH 6.0 (Table 1). The differences in extinction coefficients and shifts in λ_{max} of the mutants are reporting on their surrounding environment, but are difficult to interpret. To obtain insights about the effects of surrounding environment, the absorption spectra of *N*-acetyl-3-nitrotyrosine amide were determined in various organic solvents with 1% triethylamine (Fig. S5, Table S5). Red-shifted phenolate absorptions (440 – 458 nm) were observed in non-protic polar solvents (DMSO, DMF and acetonitrile). In contrast, in protic solvents (water, ethanol and methanol), the phenolate absorbs at shorter wavelength, 418 – 424 nm. Thus, the red shifts of NO_2Y observed at 731 and 730 may suggest a less protic environment. π-π stacking intereactions and NO_2 group orientation, however, can also affect the phenolate absorption, and theoretical studies using structures described below are ongoing to better understand the environment of each Y.

pH titration of [NO_2Y]-β2

The pH titration of [NO_2Y_{122}]-β2 was carried out between pH 7.0 – 10.0 (Fig. 6a) with the spectra from pH 7.6 - 8.6 being identical. At pH 9.0, a decrease in A_{360nm} is observed

without a corresponding increase in the region of the phenolate, 420 - 450 nm. At pH > 9.2, further decrease in absorption in the 320 – 360 nm region occurs along with an increase in the phenolate region, although no isosbestic point is apparent. The unusual absorption spectra at pHs greater than 9 for [NO_2Y_{122}]-β2 may be due to the decomosition of the diferric cluster that generates apo-β2 which then allows titration of NO_2Y_{122}. Quantitation of iron in [NO_2Y_{122}]-β2 at pH 10.0, for examle, showed complete iron loss (Table S6) and the phenolate absorption observed is close to that predicted from the pK_a of this residue in apo-β2 (see below). Thus, the pK_a of the iron loaded form (met-form) cannot be directly determined. Since the spectra between pH 7.6 - 8.6 are identical, and 10 % of phenolate would result in a detectable change in absorbance (0.007, assuming an ε = 4200 $M^{-1}cm^{-1}$), a lower limit of detection of the pK_a of the phenol can be set at 9.6. The pK_a perturbation of NO_2Y_{122} is thus greater than 2.5 pH units. Results from the titration of [NO_2Y_{122}]-β2 with wt-α2/*E*/*S* are similar to the titration without α2 (Fig. S6).

In contrast, a pH titration of NO_2Y was successfully carried out between pH 7.0 - 10.6 with apo-[NO_2Y_{122}]-β2 which does exhibit an isosbestic point (Fig. 6b). Titration above pH 10.8 was not possible due to protein precipitation. These data, fit to eq.2, gave a pK_a of 9.8. This pK_a is close to the lower limit of pK_a for the met-form (9.6), indicating that the diferric cluster does not significantly lower the phenol pK_a. The λ_{max} and the extinction coefficient of phenolate were minimally perturbed from that of *N*-acetyl-3-nitrotyrosine amide in water (Table 1).

The pK_a of [NO_2Y_{356}]-β2 was also revisited using ATP/CDP. [NO_2Y_{356}]-β2 prepared by EPL29 was used due the reduction of NO_2Y in 356 of β2 incorporated by the orthogonal tRNA/RS methodology. The pK_a with ATP/α2 and ATP/α2/CDP are very similar to the ppreviously determined pK_a with dGTP/α2/ADP (Table 4c). For all the NO_2Y mutants, ATP/CDP and dGTP/ADP gave almost identical pK_as.

pK_as of [NO_2Y]-α2s with a second mutation adjacent to NO_2Y in the PCET pathway

The crystal structure of GDP/TTP bound *E. coli* α2 indicates that the distance between the oxygens of the phenol of Y_{731} and Y_{730}-α2 is 3.3 Å and the distance between the oxygen of Y_{730}-α2 and the sulfur of C_{439}-α2 is 3.4 Å.5 The distances indicate the possibility of pH bonding interactions between these species, which likely plays an important role in PCET.[56-59] The structure also suggests an unusual π–π stacking interaction of Y_{731}- and Y_{730}-α2, which may also be of interest mechanistically, although the degree of stacking varies in recent structures of α from other sources.[60,61] Removal of a H bonding interaction or the π stacking might perturb the pK_a of the phenolic hydroxyl group. A variety of double mutants (Y to Phe/Ala and Cys to Ser/Ala) were successfully expressed and isolated. Their purity was similar to the corresponding parent single mutant (Table S4).

The λ_{max} and ε of the phenolate, and the K_d for subunit interactions for each double mutant were determined (Tables 1 and 2) and are similar to the parent single mutant. Conservative substitutions minimally perturbed the K_d, while the non-conservative substitution of Ala for C_{439} or Y_{731} in [NO_2Y_{730}]-α2 resulted in large K_d perturbations (Table 2). As noted above, all double mutants showed specific activities of 1-3% of wt-α2, similar to the single mutants and presumeably associated with endogenous wt-α2.

The pK_a of each double mutant was determined (Table 4A and 4B, Fig. S7). With [NO_2Y_{730}]-α2, Y_{731} was replaced with Phe and C_{439} with Ala, mutations that disrupt the putative H bonding. C_{439} was also relaced with Ser that could enhance H bonding. With the C_{439}A double mutant, the pK_a was increased from 7.9 to 8.3/8.4 in the presence of *E* (ATP or dGTP) or *E*/β2 and addition of *S* (CDP or ADP) again perturbed the pK_a by 0.2 to 0.3 units. With Y_{731}F, the addition of *S* also elevated the pK_a to 8.2. Only in the case of C_{439}S

did addition of substate aear to have no effect. However, as will be seen from the structures described in the following section, [NO_2Y_{730}]-α2/ C_{439}S is the only mutant in which 439 is H bonded to the active site E_{441}(Fig 7d). Thus, we propose that *S* binding would disrupt this H bonding interaction and reset the pK_a to 7.9 while *S* binding would then perturb the pK_a to 8.3 as observed with the other mutants. These studies reveal that *S* binding generally elevates the pK_a of residue 730 and that this increase is independent of pH bonding ability of the residues at 439 and 731.

Studies with [NO_2Y_{730}]-α2 and Y_{731} replaced with an Ala were also examined to address the putative importance of π–π stacking interactions. The pperturbations in pK_a for this mutant were the largest observed in any of the titrations, decreasing from 7.8/7.9 (single mutant) to 6.5 (double mutant) in the presence of E. The observed pK_as are 0.6 units lower than the *N*-acetyl-3-nitrotyrosine amide. However, even in this case, the pK_a was substantially increased, from 6.5 to 6.8/7.0, on addition of *S*. This double mutant also exhibited the largest pperturbation in K_d (Table 2) suggesting that the structure of the complex is perturbed by this non-conservative substitution.

Titration studies were also carried out with [NO_2Y_{731}]-α2 and Y_{356}F-β2 and with the double mutant where Y_{730} was replaced with F. In the former case, the pK_a, was unaffected by *S* addition. However, the pK_a of the Y_{730}F double mutant decreased 0.5 units relative to the single mutant with *E* and *E*/wt-β2 and increased back toward that of the single mutant pK_a on addition of S. The studies in sum suggest that *S* perturbs the pK_a at 730 with minimal effect at 731 and that the altered pK_as do not appear to be the result of increased H bonding by residues adjacent to the substitution.

Crystal structures of NO_2Y-α2s

Understanding the experimental data obtained with the unnatural amino acid probes in α and β requires structural information and computational efforts. As a first step toward structural characterization, crystals of wt and seven NO_2Y-α2 mutants were obtained in the presence of a 20mer peptide, identical to the C-terminal 20 amino acids of β, using crystallization conditions similar to those previously reported for wt-α2.4 The structure of wt-α2, isolated by methods similar to the NO_2Y-α2s, was solved by molecular replacement using Y_{730}F-α2 (DB ID, 1R1R).5 This new wt-α2 structure (2.3 Å resolution) was then used as the starting point to solve the NO_2Y-α2 structures, which were obtained and refined to 2.1 – 3.1 Å resolution. In all mutants, there are three α subunits in the asymmetric unit with two of the three subunits forming a dimer. The data collection methods and refinement statistics are summarized in Table S3. In general, the structures revealed minimal overall perturbation relative to the wt structure and the phenyl rings and OH groups of NO_2Ys superimosed well with the corresponding residues in the wt structure (Fig. 7). In all of the structures the distances between the oxygens of the two phenols (at 731 and 730) and of the phenol and the thiol (at 730 and 439) are very similar to the distances found in wt-α and are within H bonding distance in the former case and slightly longer than H bonding distance in the latter case.

The NO_2 group in all of the structures lies on the sterically less crowded side, the left side looking toward C_{439} from Y_{731}(Fig. 7a and 7b). At 730, the NO_2 groupp in all single and double mutants lies in the plane of the phenyl ring. No additional electron density is apparent in the vicinity of [NO_2Y_{730}]-α2 that can be associated with water. On the other hand, the NO_2 group at 731 has different orientations in each of the three αs in the asymmetric unit. In two of the αs, the NO_2 group is perpendicular to the plane of the phenyl ring, while in the remaining α, it is almost parallel to the ring. The oxygens of the NO_2 groupp have pH bonding interactions with H_2O(s), which are distinct within each α. The

double mutant ($Y_{730}F$) also has its NO_2 group perpendicular to the phenyl ring, but no waters are identifiable.

Finally a superposition of all the [NO_2Y_{730}]-α structures (Fig. 7D) shows that residue 439 adots a different conformation in the serine mutant, in which the OH of serine appears to H bond to E_{441}, a key residue in the active site involved in catalysis. The SH of Cys in the wt-α2, on the other hand, points toward residue 730. Thus, the structures in general suggest H bonding interactions are important in the PCET with C_{439} showing the greatest flexibility. The detailed analysis of the structures is ongoing and will be published subsequently. Ultimately, structures with *S*, *E* and β2 bound will be critical to understanding the role of H bonding interactions in the radical propagation process.

Discussion

Understanding of the radical propagation process in RNR requires an understanding of factors that control the different mechanisms of PCET in well-defined model systems where the rate constants for oxidation can be measured and the parameters that influence these rate constants such as H bonding, electronic effects, and the proton acceptor can be manipulated.[56,58,62-67] Different tyes of models will be required to probe PCET within β and within α of RNR (Fig. 1). H bonded phenols, for examle, have been designed to understand the oxidation of the Y_Z in photosystem II in which a histidine functions as the proton acceptor from Y_Z during its oxidation.[68,69] phenols with amine and imidazole bases[62,63,70] and carboxylates[56,65,66] appended ortho to the phenol have been synthesized and structurally and sectroscoically characterized. The rate constants for oxidation and the deuterium kinetic isotope effects on oxidation have been measured as a function of temperature.[56,62,65,66,70] The Hammarström model seems particularly appropriate for Y_{356} oxidation in RNR where E_{350} is proposed to be the initial proton acceptor (Fig. 1). However, appropriate models for the putative H bond network between $Y_{731}/Y_{730}/C_{439}$, with no obvious base proximal to either Y, are not yet available.

As a starting point to understanding the PCET in RNR, we have chosen NO_2Y and NH_2Y as reporters on the H bonding interactions of each Y in the ground states and the transient Y· intermediate states in the radical propagation process, respectively. In the former case, we proposed that the phenol pK_a might be altered by the protein environment on binding of the second subunit and/or *S/E*. In the latter case, ^1H and ^2H ENDOR sectroscoy might allow direct observation of H bond interactions to the radical intermediates.[71] The focus of this aer is NO_2Y.

To carry out these studies, the evolved tRNA/RS method pioneered by the Schultz lab[42] was optimized to site-specifically incorporate high levels of NO_2Y in place of Y_{122}, Y_{731} and Y_{730}. Our efforts to insert NO_2Y in place of Y_{356} have thus far been unsuccessful due to reduction during the expression process. The inactivity of these mutants has allowed us to determine the pK_a of each NO_2Y in the α2β2 complex in the presence of substrate (*S*) and effector (*E*), presumably in the “active” conformation required for PCET. Together with our previous pK_a data for [NO_2Y_{356}]-β2, the results presented show the ower of site-specific incorporation of unnatural amino acids to measure individual pK_as in a protein with 1135 amino acids. These measurements for four different NO_2Ys, provide an important step in understanding radical initiation in RNR.

Mechanistic insights

Our pH titration data has established that each Y in the pathway (Fig. 1) has distinct properties. The greatest pK_a perturbations are observed with NO_2Y_{122}-β2: elevations of 2.7 and >2.5 units in apo and met form, respectively. This Y is unique in that its oxidation

results in a stable Y· ($t_{1/2}$ of 4 days at 4°C) and it is generated by the metal cluster. An explanation for its unsual stability is clear from a Comparison of X-ray crystal structures of met-β26 (β2 with Y· reduced-diferric cluster), apo-β272, and Mn_2-β273 and results from single crystal high field EPR spectroscoy of the active diferric-Y·-β2.7 In the crystal structure of the class Ia Mn_2-β273 the Y_{122}-OH is within H bonding distance to D_{84}, a carboxylate ligand to Mn1 (corresponds to Fe1 in Fig. 1b) of the cluster, that in turn may H bond with a H_xO (x = 1, 2) bound to the same Mn (Fig 1b). If similar interactions exist in the diferric cluster during radical propagation in the presence of α/*S/E*, then the close interaction of the phenol with the D_{84} carboxylate, would preclude its ionization, to prevent electrostatic repulsion with D_{84}. The pK_a of 9.8 for NO_2Y in apo-[NO_2Y_{122}]-β2 suggests that its environment, even in the apo form, is very hydrophobic (Q_{80}, I_{231}, I_{234}, F_{208}, L_{77}, F_{212}, Fig. S8). On the other hand, high field EPR spectroscopy of active β2 (Y·) reveals that this Y_{122} is no longer H bonded.7 Our current model is that only subsequent to *S/E* binding in α is PCET initiated and the Y· reoriented toward D_{84} so that it can pick u a proton from the H_2O bound to Fe1 concomitant with its reduction by W_{48}.12,14,15 Thus, the environment of the Y· is such that it is stable, unless a proton is also available. The elevated pK_a of NO_2Y observed in our titrations is consistent with concerted PCET mechanism for Y_{122} oxidation in which the proton donor is distinct from the reductant (W_{48}).

The pK_as of NO_2Y at 356 in β2 and 730 and 731 in α2 are pperturbed to a much smaller extent than at 122 with perturbations increasing as the distance of the Y increases from Y_{122} (7.5,74 7.9, 8.3 for NO_2Y 356, 731 and 730, respectively). The perturbation ranges from 0.4 to 1.2 units relative to NO_2Y within the 20mer-C-terminal peptide. These measurements demonstrate that Nature has pEVOLved a different tye of environment for transient radical formation and a different mechanism for their oxidation. pK_a at each transient Y· site is discussed.

Studies in a variety of enzymes containing redox cofactors have established that binding of substrate provides a mechanism to perturb the reduction potential of the cofactor, and to facilitate the chemistry.75,76 We thus investigated whether the addition of the correct *S/E* air to RNR could alter the pK_a of each Y and provide insight about its oxidation mechanism. The pK_a of NO_2Y_{730} is uniquely increased by 0.4 units on addition of either a purine or pyrimidine substrate to the [NO_2Y_{730}]-α2/β2/*E*. The basis for this perturbation and the potential importance of the H bond network was investigated by titration studies with double mutants that have altered H bonding capabilities in residues adjacent to NO_2Y_{730}-α2. The parallel NO_2 group orientation relative to the plane of the phenyl group with all mutants suggests that relative pK_as are informative. In all cases excet $C_{439}S$, addition of substrate elevates the pK_a regardless of the H bonding interactions, consistent with an increased hydrohobic environment. No waters are identifiable in the region surrounding 730. The observations with the Ser mutant can also be rationalized as described in the Results. At present, we do not know if this small perturbation is mechanistically important or why the pK_a is increased. Finally, it is also likely that if H bonding is key to the mechanism of the thiyl radical generation, it may be manifested predominantly in the transition states of the reaction and may not be readily apparent from this type of groupnd-state analysis.15,65

The two remaining Ys (Fig 1) are located at the subunit interface and unfortunately no structural information is available for the active α2β2 complex. Our studies, however, with 3,5-F_2Y at Y_{356} revealed that nucleotide reduction can occur through the phenolate form of this residue, consistent with non-obligate coupling of the electron and proton transfer and with the proton transfer occuring orthogonal to the ET pathway.21 The minimal perturbation of the NO_2Y pK_a at this position suggests it may be more solvent exposed in the complex than Y_{730}, which is also consistent with our recent studies using an environmentally sensitive fluorophore attached at 356.54 Our current hyothesis for PCET at this position is

that orthogonal PCET occurs with transfer of a proton to E_{350} within the C-terminal tail of β. The importance of this residue in nucleotide reduction was demonstrated by previous studies of Climent et al.16 with a E_{350}A mutant and our recent studies with E_{350}Q mutant (unublished results). As noted above, the model studies of Hammarström may thus provide a model of PCET at this center.56,66

The pK_a of NO_2Y_{731} and its minimal perturbation in double mutants with Y_{356}F and Y_{730}F, suggests that a H bonding is again not observable at this position and that this residue may be solvent exposed. The structure of the single mutant shows that the NO_2 group is more flexible at this position with conformations both parallel and perpendicular to the plane of the phenyl ring and that it H bonds with specific water molecules that are distinct in each α. Sequence analysis of conserved residues of RNR with the constraint that they reside within the subunit interface based on the docking model,4 reveal only E_{350} and R_{236} in β and no interesting conserved residues in α. Studies on R_{265} mutants in mouse β, corresponding to the R_{236} mutant in *E. coli* β, have been interpreted to support a role for this residue in the proton coupling in the propagation pathway.77 However, since R_{265}E mutant exhibited 40% the activity of the wt enzyme, it is unlikely to function as a proton acceptor. Unfortunately, interactions that are proposed to be important in our models for radical propagation in RNR (Fig. 1)14,15 are not apparent from the pK_a measurements. Our studies suggest that the pK_as of the Ys that undergo transient oxidations during radical propagation in RNR do not aear to be significantly perturbed. Comutational efforts are underway to use the structural information to understand the pK_a perturbations.

Summary

Desite the prevalence of PCET in biological systems, pK_a information of individual redox active residues in proteins is scarce. A general method for directly measuring the pK_a of a single residue within a protein would be mechanistically useful.78 In this paper NO_2Y has been used as a probe to measure the pK_a perturbations of the all redox-active Ys, 122- and 35674-β2, 731- and 730-α2, in the radical propagation pathway in *E.coli* RNR. The crystal structures of the NO_2Y-α2 mutants have shown minimal structural perturbations. The pH titrations have shown position dependent pK_a perturbations at these redox active Y sites with the largest and distinct perturbation at the stable tyrosyl radical site, Y_{122}-β2. The study reveals distinct environments for the stable and transient Y·. The pK_a information reported is essential to understand the mechanism of long range PCET in RNR.

Supplementary Material

Refer to Web version on PubMed Central for supplementary material.

Acknowledgments

We thank Ellen C. Minnihan for helpful discussions. This work was supported by the NIH grant GM29595 to J. S.

This work was supported by the NIH grant GM29595 (to JS).

References

(1). Stubbe J, van der Donk WA. Chem. Rev. 1998; 98:705–762. [PubMed: 11848913]

(2). Jordan A, Reichard P. Annu. Rev. Biochem. 1998; 67:71–98. [PubMed: 9759483]

(3). Nordlund P, Reichard P. Annu. Rev. Biochem. 2006; 75:681–706. [PubMed: 16756507]

(4). Uhlin U, Eklund H. Nature. 1994; 370:533–539. [PubMed: 8052308]

(5). Eriksson M, Uhlin U, Ramaswamy S, Ekberg M, Regnstrom K, Sjöberg B-M, Eklund H. Structure. 1997; 5:1077–1092. [PubMed: 9309223]

(6). Nordlund P, Sjöberg B-M, Eklund H. Nature. 1990; 345:593–598. [PubMed: 2190093]

(7). Högbom M, Galander M, Andersson M, Kolberg M, Hofbauer W, Lassmann G, Nordlund- P, Lendzian P. Proc. Natl. Acad. Sci. U. S. A. 2003; 100:3209–3214. [PubMed: 12624184]

(8). Uppsten M, Farnegardh M, Domkin V, Uhlin U. J. Mol. Biol. 2006; 359:365–377. [PubMed: 16631785]

(9). Marcus RA, Sutin N. Biochim. Biophys. Acta. 1985; 811:265–322.

(10). Moser CC, Keske JM, Warncke K, Farid RS, Dutton PL. Nature. 1992; 355:796–802. [PubMed: 1311417]

(11). Gray HB, Winkler JR. Annu. Rev. Biochem. 1996; 65:537–561. [PubMed: 8811189]

(12). Siegbahn PEM, Eriksson L, Himo F, Pavlov M. J. Phys. Chem. B. 1998; 102:10622–10629.

(13). Ekberg M, Sahlin M, Eriksson M, Sjöberg B-M. J. Biol. Chem. 1996; 271:20655–20659. [PubMed: 8702814]

(14). Reece SY, Hodgkiss JM, Stubbe J, Nocera DG. Phil. Trans. R. Soc. B. 2006; 361:1351–1364. [PubMed: 16873123]

(15). Stubbe J, Nocera D, Yee CS, Chang MCY. Chem. Rev. 2003; 103:2167–2201. [PubMed: 12797828]

(16). Climent I, Sjöberg B-M, Huang CY. Biochemistry. 1992; 31:4801–4807. [PubMed: 1591241]

(17). Ekberg M, Birgander P, Sjöberg B-M. J. Bacteriol. 2003; 185:1167–1173. [PubMed: 12562785]

(18). Seyedsayamdost MR, Stubbe J. J. Am. Chem. Soc. 2006; 128:2522–2523. [PubMed: 16492021]

(19). Seyedsayamdost MR, Yee CS, Reece SY, Nocera DG, Stubbe J. J. Am. Chem. Soc. 2006; 128:1562–1568. [PubMed: 16448127]

(20). Seyedsayamdost MR, Reece SY, Nocera DG, Stubbe J. J. Am. Chem. Soc. 2006; 128:1569–1579. [PubMed: 16448128]

(21). Yee CS, Chang MC, Ge J, Nocera DG, Stubbe J. J. Am. Chem. Soc. 2003; 125:10506–10507. [PubMed: 12940718]

(22). DiLabio GA, Johnson ER. J. Am. Chem. Soc. 2007; 129:6199–6203. [PubMed: 17444643]

(23). Seyedsayamdost MR, Xie J, Chan CT, Schultz PG, Stubbe J. J. Am. Chem. Soc. 2007; 129:15060–15071. [PubMed: 17990884]

(24). Minnihan EC, Seyedsayamdost MR, Stubbe J. Biochemistry. 2009; 48:12125–12132. [PubMed: 19916558]

(25). Chang MC, Yee CS, Stubbe J, Nocera DG. Proc. Natl. Acad. Sci. U. S. A. 2004; 101:6882–6887. [PubMed: 15123822]

(26). Reece SY, Seyedsayamdost MR, Stubbe J, Nocera DG. J. Am. Chem. Soc. 2007; 129:8500–8509. [PubMed: 17567129]

(27). Reece SY, Seyedsayamdost MR, Stubbe J, Nocera DG. J. Am. Chem. Soc. 2007; 129:13828–13830. [PubMed: 17944464]

(28). Pesavento RP, van der Donk WA. Adv. Protein Chem. 2001; 58:317–385. [PubMed: 11665491]

(29). Yee CS, Seyedsayamdost MR, Chang MC, Nocera DG, Stubbe J. Biochemistry. 2003; 42:14541–14552. [PubMed: 14661967]

(30). Rived F, Rosés M, Bosch E. Anal. Chim. Acta. 1998; 374:309–324.

(31). Maran F, Celadon MG, Severin E, Vianello E. J. Am. Chem. Soc. 1991; 113:9320–9329.

(32). Izutsu, K. Acid-base dissociation constants in dipolar aprotic solvents. Blackwell Scientific Publications; Oxford: 1990.

(33). Bosch E, Roses M. Talanta. 1989; 36:627–632. [PubMed: 18964770]

(34). Bosch E, Rafols M, Roses M. Talanta. 1989; 36:1227–1231. [PubMed: 18964895]

(35). Neumann H, Hazen JL, Weinstein J, Mehl RA, Chin JW. J. Am. Chem. Soc. 2008; 130:4028–4033. [PubMed: 18321101]

(36). Chivers PT, Prehoda KE, Volkman BF, Kim BM, Markley JL, Raines RT. Biochemistry. 1997; 36:14985–14991. [PubMed: 9398223]

(37). Pigiet VP, Conley RR. J. Biol. Chem. 1977; 252:6367–6372. [PubMed: 330529]

(38). Salowe SP, Stubbe J. J. Bacteriol. 1986; 165:363–366. [PubMed: 3511029]

(39). Salowe SP, Ator MA, Stubbe J. Biochemistry. 1987; 26:3408–3416. [PubMed: 3307907]

(40). Thelander L. J. Biol. Chem. 1973; 248:4591–4601. [PubMed: 4578086]

(41). Atkin CL, Thelander L, Reichard P, Lang G. J. Biol. Chem. 1973; 248:7464–7472. [PubMed: 4355582]

(42). Wang J, Brock A, Herberich B, Schultz PG. Science. 2001; 292:498–500. [PubMed: 11313494]

(43). Young TS, Ahmad I, Yin JA, Schultz PG. J. Mol. Biol. 2010; 395:361–374. [PubMed: 19852970]

(44). Mao SS, Johnston MI, Bollinger JM, Stubbe J. Proc. Natl. Acad. Sci. U. S. A. 1989; 86:1485–1489. [PubMed: 2493643]

(45). Farrell IS, Toroney R, Hazen JL, Mehl RA, Chin JW. Nat. Methods. 2005; 2:377–384. [PubMed: 16170867]

(46). Berglund O, Eckstein F. Methods Enzymol. 1974; 34:253–261. [PubMed: 4615236]

(47). Hristova D, Wu CH, Jiang W, Krebs C, Stubbe J. Biochemistry. 2008; 47:3989–3999. [PubMed: 18314964]

(48). Fish WW. Methods Enzymol. 1988; 158:357–364. [PubMed: 3374387]

(49). Climent I, Sjöberg B-M, Huang CY. Biochemistry. 1991; 30:5164–5171. [PubMed: 2036382]

(50). Hammill JT, Miyake-Stoner S, Hazen JL, Jackson JC, Mehl RA. Nat. Protoc. 2007; 2:2601–2607. [PubMed: 17948003]

(51). The presence of 6 M guanidine HCl perturbed λ_{max} as well as the extinction coefficient of N-acetyl-3-nitrotyrosine.

(52). Balabanli B, Kamisaki Y, Martin E, Murad F. Proc. Natl. Acad. Sci. U. S. A. 1999; 96:13136–13141. [PubMed: 10557286]

(53). Baldwin J, Krebs C, Ley BA, Edmondson DE, Huynh BH, Bollinger JM. J. Am. Chem. Soc. 2000; 122:12195–12206.

(54). Hassan AQ, Wang Y, Plate L, Stubbe J. Biochemistry. 2008; 47:13046–13055. [PubMed: 19012414]

(55). Ge J, Yu G, Ator MA, Stubbe J. Biochemistry. 2003; 42:10071–10083. [PubMed: 12939135]

(56). Sjödin M, Irebo T, Utas JE, Lind J, Merényi G, Åkermark B, Hammarström L. J. Am. Chem. Soc. 2006; 128:13076–13083. [PubMed: 17017787]

(57). Skone JH, Soudackov AV, Hammes-Schiffer S. J. Am. Chem. Soc. 2006; 128:16655–16663. [PubMed: 17177415]

(58). Ludlow MK, Skone JH, Hammes-Schiffer S. J. Phys. Chem. B. 2008; 112:336–343. [PubMed: 17939710]

(59). Mayer JM, Hrovat DA, Thomas JL, Borden WT. J. Am. Chem. Soc. 2002; 124:11142–11147. [PubMed: 12224962]

(60). Xu H, Faber C, Uchiki T, Fairman JW, Racca J, Dealwis C. Proc Natl Acad Sci U S A. 2006; 103:4022–4027. [PubMed: 16537479]

(61). Uppsten M, Färnegardh M, Jordan A, Eliasson R, Eklund H, Uhlin U. J. Mol. Biol. 2003; 330:87–97. [PubMed: 12818204]

(62). Markle TF, Rhile IJ, Dipasquale AG, Mayer JM. Proc. Natl. Acad. Sci. U. S. A. 2008; 105:8185–8190. [PubMed: 18212121]

(63). Rhile IJ, Markle TF, Nagao H, Dipasquale AG, Lam OP, Lockwood MA, Rotter K, Mayer JM. J. Am. Chem. Soc. 2006; 128:6075–6088. [PubMed: 16669677]

(64). Mayer JM. Annu. Rev. Phys. Chem. 2004; 55:363–390. [PubMed: 15117257]

(65). Johannissen LO, Irebo T, Sjödin M, Johansson O, Hammarström L. J. Phys. Chem. B. 2009; 113:16214–16225. [PubMed: 20000384]

(66). Irebo T, Johansson O, Hammarström L. J. Am. Chem. Soc. 2008; 130:9194–9195. [PubMed: 18582051]

(67). Hammes-Schiffer S, Soudackov AV. J. Phys. Chem. B. 2008; 112:14108–14123. [PubMed: 18842015]

(68). Lomoth R, Magnuson A, Sjödin M, Huang P, Styring S, Hammarström L. Photosynth. Res. 2006; 87:25–40. [PubMed: 16416050]

(69). Mayer JM, Rhile IJ, Larsen FB, Mader EA, Markle TF, DiPasquale AG. Photosynth. Res. 2006; 87:3–20. [PubMed: 16437185]

(70). Markle TF, Mayer JM. Angew. Chem. Int. Ed. 2008; 47:738–740.

(71). Seyedsayamdost MR, Argirević T, Minnihan EC, Stubbe J, Bennati M. J. Am. Chem. Soc. 2009; 131:15729–15738. [PubMed: 19821570]

(72). Aberg A, Nordlund P, Eklund H. Nature. 1993; 361:276–278. [PubMed: 8423856]

(73). Högbom M, Andersson ME, Nordlund P. J. Biol. Inorg. Chem. 2001; 6:315–323. [PubMed: 11315567]

(74). pK_a of NO_2Y_{356}-β 2 was determined using the mutant preared by EPL, which requires two additional mutations, $V_{353}G$ and $S_{354}C$, that reduce the activity to 25% of the wt activity.

(75). Sligar SG, Gunsalus IC. Proc Natl Acad Sci U S A. 1976; 73:1078–1082. [PubMed: 1063390]

(76). Stankovich MT, Soltysik S. Biochemistry. 1987; 26:2627–2632. [PubMed: 3607039]

(77). Nárvaez AJ, Voevodskaya N, Thelander L, Gräslund A. J Biol Chem. 2006; 281:26022–26028. [PubMed: 16829694]

(78). Hay S, Westerlund K, Tommos C. Biochemistry. 2005; 44:11891–11902. [PubMed: 16128591]

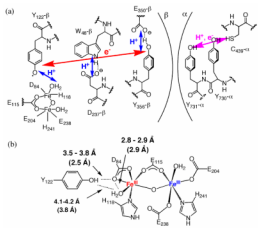

Figure 1.

Tyrosines responsible for the PCET in *E. coli* class I RNR. (a) Proposed PCET pathway. Red and blue arrows indicate orthogonal transfer of the electron and proton, respectively. The purple arrow indicates co-linear movement of the electron and proton. (b) Structure of the tyrosine-diferric-cluster.6 Distances in parentheses are those of the Mn_2-β2.73

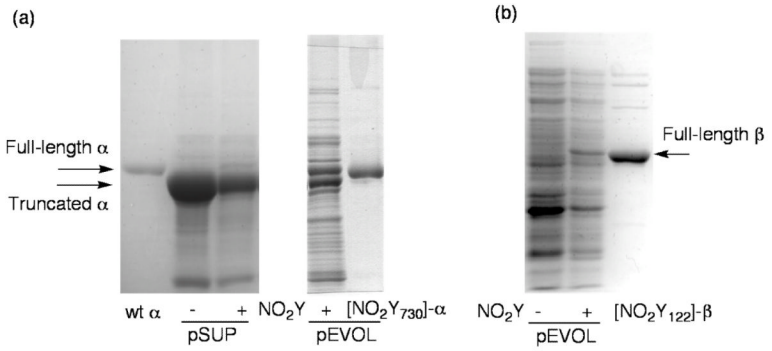

Figure 2.

SDS-PAGE of $[NO_2Y_{730}]$-α and $[NO_2Y_{122}]$-β. (a) SDS-PAGE of purified $[NO_2Y_{730}]$-α and whole cell lysate of *E. coli* expressing $[NO_2Y_{730}]$-α using pSUP-3NT/8 (left) and pEVOL-NO_2Y (right). Cells were grown in the presence or absence of NO_2Y as indicated. The position of protein bands for full-length α (85.6 kDa) and truncated α (82.2 kDa) are denoted by arrows. (b) SDS-PAGE of purified $[NO_2Y_{122}]$-β (45.0 kDa) and a whole cell lysate of *E. coli* TOP10/pEVOL-NO_2Y/pBAD-*nrdB*-NS5-$Y_{122}Z$ grown in the absence and presence of NO_2Y as indicated. The truncated protein is 15.9 kDa and thus not observable in this gel (10 % acrylamide).

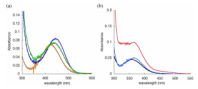

Figure 3.

Absorption spectra of nitrophenolate feature of [NO_2Y]-α2s and nitrophenol feature of [NO_2Y_{122}]-β2. (a) [NO_2Y_{730}]-α2 (blue), [NO_2Y_{731}]-α2 (green) and *N*-acetyl-3-nitrotyrosine amide (yellow) in 50 mM TAPS (pH 9.0), 1 mM EDTA, 15 mM $MgSO_4$. Spectral intensities were normalized to NO_2Y concentration (15 μM) according to the purity of [NO_2Y_{730}]-α2 (92%), [NO_2Y_{731}]-α2 (79%) determined from A_{435nm} in 6 M guanidine. (b) Red trace, absorption spectra of [NO_2Y_{122}]-β2 (2.9 Fe/β2, 15 μM) in HEPES (pH 7.6); blue trace, absorption spectrum after subtraction of the met-β2 spectrum (3.2 Fe/β2, 13.5 μM, the concentration of β2 was normalized for the iron content); black trace, absorption spectrum of *N*-acetyl-3-nitrotyrosine amide in 50 mM MES (pH 5.0) buffer.

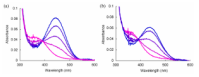

Figure 4.

UV-vis absorption spectra of (a) [NO_2Y_{730}]-α2 (7.5 μM) and (b) [NO_2Y_{731}]-α2 (7.5 μM) at pH 6.0 (the pink trace), 7.4, 8.0, 8.6 and 9.2 (the blue trace) in the presence of 1 mM ATP. Loss of the phenol feature (360 nm) occurs concomitant with the formation of the phenolate feature (442 and 437 nm for [NO_2Y_{730}]-α2 and [NO_2Y_{731}]-α2, respectively) with increasing pH (pink to blue).

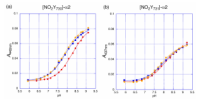

Figure 5.
Titration curves of (a) [NO_2Y_{730}]-α2 and (b) [NO_2Y_{731}]-α2 in the presence of 1 mM ATP (yellow diamonds), 1 mM ATP and 7.5 μM β2 (blue squares) and 1 mM ATP, 7.5 μM β2 and 1 mM CDP (red circles). Absorption at 442 nm and 437 nm were monitored for [NO_2Y_{730}]-α2 and [NO_2Y_{731}]-α2, respectively. Each data point prepresents an average of three replicates. Lines are from fits to eq. 2.

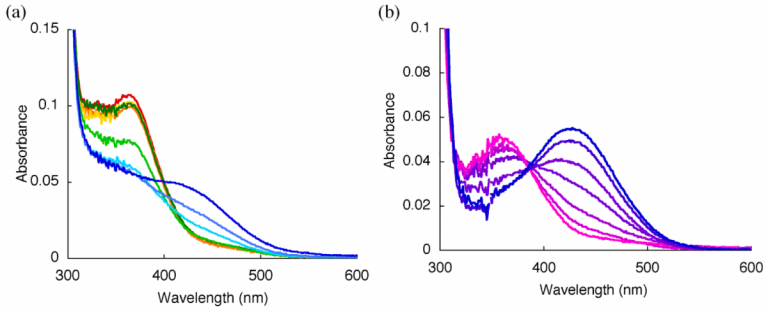

Figure 6.

UV-vis absorption spectra of (a) met-[NO_2Y_{122}]-β2 at pH 7.1 (red), 7.6 (orange), 8.2 (yellow), 8.6 (dark green), 9.0 (light green), 9.2 (light blue), 9.5 (blue) and 10.0 (dark blue), and (b) apo-[NO_2Y_{122}]-β2 at pH 7.6 (the pink trace), 8.4, 9.0, 9.6, 10.0, 10.3 and 10.6 (the blue trace).

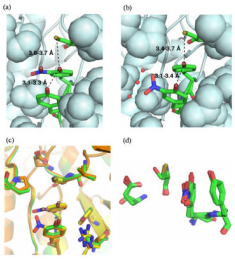

Figure 7.

Crystal structures of the radical propagation pathway in NO_2Y-α2 mutants. The crystals were grown at pH 6.0-6.5. Oxygens are colored in red, nitrogens in blue, and sulfurs in gold. Pathway residues 731, 730 and 439 are shown with sticks. The structure of (a) [NO_2Y_{730}]-α2 and (b) [NO_2Y_{731}]-α2; the dotted lines indicate the distances between the phenolic oxygens, and the phenolic oxygen of the 730 residue and the sulfur of C_{439} with distance variations associated with the three subunits in the asymmetric unit. The surrounding residues are shown as sheres. (c) An overlay of the structures of wt-α2 (green), [NO_2Y_{730}]-α2 (orange), and [NO_2Y_{731}]-α2 (yellow), generated using PyMOL 1.1 (DeLano Scientific LLC) software. Other residues shown are P_{621}, E_{441}, L_{438}, Y_{413} and R_{411}. (d) An overlay of the structures of [NO_2Y_{730}]-α2 and the double mutants $C_{439}S$, $C_{439}A$, $Y_{731}A$ and $Y_{731}F$. Residues shown are (from the left) 441, 439, 730 and 731.

Table 1

Extinction coefficients of NO_2Y phenol and phenolate in RNR

	phenol		Phenolate	
	λ_{max}	ε ($M^{-1}cm^{-1}$)[b]	λ_{max}	ε ($M^{-1}cm^{-1}$)[a]
N-Ac-NO_2Y-NH_2	360 nm	2960	424 nm	4610
[NO_2Y_{730}]-α2	360 nm	3800 ± 170	442 nm	6400 ± 250
[NO_2Y_{731}]-α2	360 nm	4200 ± 300	437 nm	5200 ± 300
[NO_2Y_{730}]-α2(Y_{731}F)	360 nm	3400 ± 160	445 nm	6200 ± 210
[NO_2Y_{730}]-α2(Y_{731}A)	360 nm	4100 ± 200	435 nm	7000 ± 200
[NO_2Y_{730}]-α2(C_{439}S)	360 nm	3700 ± 220	442 nm	6800 ± 240
[NO_2Y_{730}]-α2(C_{439}A)	360 nm	3400 ± 230	442 nm	6000 ± 220
[NO_2Y_{731}]-α2(Y_{730}F)	360 nm	4000 ± 230	437 nm	5900 ± 150
[NO_2Y_{122}]-β2 (met form)	363 nm	3400 ± 240[c]	nd	nd
[NO_2Y_{122}]-β2 (apo form)	363 nm	3400 ± 240	425 nm	4200 ± 220

[a] Extinction coefficients of phenolates were determined from pH titration curve fitting to eq.2. The titration curves were generated by plotting absorbance at indicated phenolate λ_{max} as a function of pH. Titration curves used are shown in Fig. 5 and Fig. S7.

[b] Extinction coefficients of phenol were calculated from the UV-vis spectrum at pH 6.0.

[c] The extinction coefficients of [NO_2Y_{122}]-β2 (met form) was determined from the absorption spectrum at pH 7.6 after subtracting a spectrum of wt met-β2 normalized by the iron content.

Table 2

K_d of [NO_2Y]-α2s with wt-β2 or [NO_2Y_{122}]-β2 with wt-α2

	K_d (μM)[a]
[NO_2Y_{730}]-α2	1.32 ± 0.10
[NO_2Y_{731}]-α2	0.51 ± 0.07
[NO_2Y_{730}]-α2(Y_{731}F)	1.45 ± 0.14
[NO_2Y_{730}]-α2(Y_{731}A)	2.71 ± 0.13
[NO_2Y_{730}]-α2(C_{439}S)	1.28 ± 0.07
[NO_2Y_{730}]-α2(C_{439}A)	2.07 ± 0.07
[NO_2Y_{731}]-α2(Y_{730}F)	0.50 ± 0.04
[NO_2Y_{122}]-β2	0.40 ± 0.06

[a] K_d was determined at pH 7.6 by using [NO_2Y]-α2s or [NO_2Y_{122}]-β2 as competitive inhibitors of CDP reduction by α2, β2, TR, TRR and NADPH.49

Table 3

RNR activities of [NO_2Y]-α2s and [NO_2Y_{122}]-β2

	Radioactive RNR assay (%wt) [a]	Spectrophotometric RNR assay (%wt) [a]	Yield (mg/g)
[NO_2Y_{730}]-α2	1.1	1.5	2.8
His-[NO_2Y_{730}]-α2[b,c]	0.5	0.5	5.8
[NO_2Y_{731}]-α2	2.9	3.1	1
[NO_2Y_{731}]-α2[b]	0.6	0.4	2.4
[NO_2Y_{730}]-α2(Y_{731}F)	2.5	2.7	0.8
[NO_2Y_{730}]-α2(Y_{731}A)	1.8	2.0	1.4
[NO_2Y_{730}]-α2(C_{439}S)	2.4	2.6	1.1
[NO_2Y_{730}]-α2(C_{439}A)	2.7	2.8	0.8
[NO_2Y_{731}]-α2(Y_{730}F)	1.7	1.3	2
[NO_2Y_{122}]-β2[b,d]	0.39	0.29	7
[NO_2Y_{122}]-β2[b,e]	> 0.01	> 0.1	0.4

[a] Activities are reported as % activity of wt α2 (2500 nmol/min/mg) or wt β2 (6500 nmol/min/mg).

[b] Expressed using pEVOL-NO_2Y.

[c] His-tagged NrdA purified with Ni-NTA column chromatography. See Experimental section for detail.

[d] Purified using DEAE and Q-sepharose.

[e] Purified using *strep*-Tactin sepharose.

Table 4A

pK_a of [NO_2Y_{730}]-α2 and related double mutants

	[NO_2Y_{730}]-α2	[NO_2Y_{730}]-α2 (Y_{731}F)	[NO_2Y_{730}]-α2 (C_{439}S)	[NO_2Y_{730}]-α2 (C_{439}A)	[NO_2Y_{730}]-α2 (Y_{731}A)
ATP	7.9	7.9	8.3	8.3	6.5
ATP/β2	7.9	7.9	8.4	8.3	6.6
ATP/β2/CDP	8.3	8.2	8.3	8.5	7.0
dGTP	7.8	7.9	8.4	8.3	6.5
dGTP/β2	7.8	7.9	8.5	8.4	6.5
dGTP/β2/ADP	8.2	8.2	8.4	8.6	6.8

pK_as were determined by fitting eq.2 to the pH titration curve generated by plotting phenolate absorption intensities as a function of pH. Measurements were carried out in the presence of *E*, *E*/β2 and *E*/β2/*S* and performed in triplicate. Errors were ± 0.05 pH units.

Table 4B

pK_a of [NO_2Y_{731}]-α2 and [NO_2Y_{731}]-α2($Y_{730}F$)

	[NO_2Y_{731}]-α2	[NO_2Y_{731}]-α2 ($Y_{730}F$)	[NO_2Y_{731}]-α2 /$Y_{356}F$-β2
ATP	7.9	7.4	-
ATP/β2	8.0	7.4	7.8
ATP/β2/CDP	8.0	7.7	7.8
dGTP	7.9	7.4	-
dGTP/β2	8.0	7.5	7.9
dGTP/β2/ADP	7.9	7.7	7.9

pK_as were determined as described in the footnote of Table 4A. Titrations were carried out in the presence of *E*, *E*/β2 and *E*/β2/*S* and performed in triplicate. Errors were ± 0.05 pH units

Table 4C

pK_a of [NO_2Y_{356}]-β2

	[NO_2Y_{356}]-β2
-	7.1[a]
α, α2[b]	7.2[a]
ATP/α2	7.4
ATP/α2/CDP	7.5
dGTP/α2/ADP	7.3[a]

[NO_2Y_{356}]-β2 was prepared by EPL and its pK_as were determined as described previously.29 Titrations were carried out in the presence of *E*/α2 and *E*/α2/*S* and performed in triplicate. Errors were ± 0.05 pH units.

[a] Values reported previously.29

[b] α is in equilibrium between monomer and dimer without nucleotides.40